J Mater Sci (2011) 46:1487–1493
DOI 10.1007/s10853-010-4950-1

# Growth of carbon nanotubes on aluminium foil for supercapacitors electrodes

**Reza Kavian · Antonello Vicenzo · Massimiliano Bestetti**

Received: 9 April 2010 / Accepted: 23 September 2010 / Published online: 9 October 2010


**Abstract** A new approach for the preparation of carbon nanotubes (CNTs) electrode is proposed in the present work. Multi-walled carbon nanotubes (MWCNTs) were grown by chemical vapour deposition on aluminium strips pre-plated with a nickel thin film as the catalyst. The CNTs were characterized by scanning and transmission electron microscopy, Brunauer–Emmett–Teller surface area measurement and thermogravimetric analysis. The nickel-plated aluminium foil with a layer of CNTs was further characterized for an assessment of its electrochemical behaviour as electrode for supercapacitors. The specific capacitances of the electrode, as derived from cyclic voltammetry measurement at 0.1 V $s^{-1}$ scan rate, was found to be 54 and 79 F $g^{-1}$ in aqueous and organic electrolytes, respectively, in line with the highest reported values for either activated carbon or MWCNTs electrodes. Further evidence in support of the viability of the present approach for the preparation of a CNTs electrode was obtained from electrochemical impedance spectroscopy.

## Introduction

Electrochemical supercapacitors, also known as ultracapacitors, are electrical energy storage devices exploiting the charging and discharging of the electrochemical double layer for storage and release of energy [1]. The mechanism of charge storage entails substantial advantages over conventional dielectric capacitors, such as a very high capacitance (up to 5,000 F, [2]), energy density (30 Wh $kg^{-1}$, [3]) and longer cycle life [3]. Consequently, supercapacitors have been intensively investigated for a wide range of applications from electric vehicle propulsion to power levelling and balancing [4].

Commercial supercapacitors are of two types: (1) electric double layer capacitors (EDLC) based on carbon materials and (2) faradic pseudo-capacitors based on metal oxides and conducting polymers. In the family of carbon materials, carbon nanotubes (CNTs) are considered suitable materials for the manufacture of supercapacitors due to their high porosity and specific surface area, electrical conductivity and chemical stability [5, 6].

Two types of CNTs electrodes have been so far developed for the application in supercapacitors: binder free [7] and with binder [8]. Another promising research direction involves the development of CNT/conductive polymer composite [9, 10].

The following steps are usually carried out for the preparation of CNTs electrodes: (1) functionalization of CNT; (2) dispersion of CNT in a matrix; (3) assembly of the electrode by spreading the paste containing CNT onto a metal current lead; and (4) thermal treatment. In the binder free electrode, CNTs are loosely attached to the current lead and this affects the mechanical stability and the electrical connection. On the other hand, the use of a binder can bring impurities into the electrode and impairs the electrical performance [11]. Furthermore, both methods result in a high contact resistance between the active material and the metallic substrate. Lowering the contact resistance between the CNTs and current collector in EDLC is a major issue in developing CNT-based supercapacitors [2]. In this respect, the growth of CNTs directly on the metallic substrate is obviously believed to be a promising approach to face both the problem of

R. Kavian · A. Vicenzo · M. Bestetti (✉)
Dipartimento di Chimica, Materiali e Ingegneria Chimica "G. Natta", Politecnico di Milano, Via Mancinelli 7, 20131 Milan, Italy
e-mail: massimiliano.bestetti@polimi.it

adhesion and that of the contact resistance between the CNT layer and the substrate. However, the later benefit in particular has yet to be proven either because there is not a straightforward way to manufacture such an CNT electrode, without resorting to more complex and possibly economically unattractive processes, or because even the recent advances in understanding of the intricate phenomenology of carbon-based porous electrodes for supercapacitors still do not justify such high expectations.

This article reports on the direct growth of CNTs by chemical vapour deposition (CVD) on pure aluminium foils. As the growth of CNT is catalyzed by means of transition metal nanoparticles, a thin layer of nickel was deposited on the aluminium surface before the CVD of CNTs. The CNT electrodes were characterized with regard to purity, morphology, porosity and surface area, and electrochemical behaviour.

To the author's knowledge, there have been no previous reports on the direct growth of CNT on nickel-plated aluminium current collector. A similar approach was previously attempted by direct growth of CNTs on anodically oxidized aluminium [12, 13] and cobalt sputtered graphite substrate [14]. In addition to lower ohmic losses and possibly higher specific capacitance, further advantages can be expected from this approach to the manufacture of CNTs electrodes, namely a good mechanical strength and the absence of a binder additive.

## Experimental details

### Deposition of Ni catalyst

A nickel sulphamate solution was used for nickel electrodeposition. Bath composition and operating conditions are listed in Table 1. Deposition of nickel was carried out on 2 ×2 cm highly pure aluminium in a 250 mL Pyrex beaker with magnetic stirrer and automatic temperature control unit. Current was supplied to the cell by means of a potentiostat (AMEL Mod. 549). The electrolyte pH was adjusted by addition of either sodium hydroxide or sulphamic acid to pH 4 or 2. Before electrodeposition, the aluminium substrate was degreased with acetone, rinsed with distilled water, activated by immersion in 0.1 M NaOH and finally thoroughly rinsed with distilled water. After electrodeposition, deposits were cleaned with water and dried with nitrogen gas. Nickel electrodeposition tests were performed in a range of different conditions, changing the electrolyte pH, the current density, the temperature and the deposition time, as detailed in Table 1. All the nickel-coated aluminium samples were further tested for CNT growth.

**Table 1** Electrolyte composition and operating conditions for electrodeposition of Ni

| | |
|---|---|
| Electrolyte | 110 g $L^{-1}$ nickel sulphamate, 36 g $L^{-1}$ boric acid, 0.5 g $L^{-1}$ sodium lauryl sulphate |
| pH | 2 or 4 |
| Temperature/°C | 40, 50, 60 and 70 |
| Time/min | 5, 10, 15, 20 |
| Current density/mA $cm^{-2}$ | 10, 20, 30 and 40 |
| Substrate | Al foil, 99.995%, 2 × 2 cm, thickness 130 μm |

### CNT growth

Multi-walled carbon nanotubes (MWCNTs) were grown on the nickel-coated aluminium substrate by CVD, as described in detail in a previous work [15]. The reactor was a vertical quartz tube heated in a temperature controlled furnace (Carbolite, mod. Endotherm VST 24-16). The aluminium strip covered with nickel catalyst thin film was placed vertically on a porous type P2 gas distributer in the quartz tube (ISO 4793-1980) (Fig. 1). Ethylene ($C_2H_2$) was used as carbon source. Initially, a mixture of $H_2/N_2$ ($N_2$ 500 $cm^3$ $min^{-1}$, $H_2$ 500 $cm^3$ $min^{-1}$) was fed to the reactor. The furnace temperature was increased at approximately 15 °C $min^{-1}$ up to 600 °C. As the temperature was stabilized, the flow rate of the $C_2H_2$ reactant was adjusted to its value (100 $cm^3$ $min^{-1}$) and fed to the reactor together with the $H_2/N_2$ mixture for 10 min to grow MWCNT. Finally, the reactor was flushed with nitrogen gas and cooled down to room temperature.

The amount of CNT deposited per unit area of the substrate was determined by measuring the mass change of

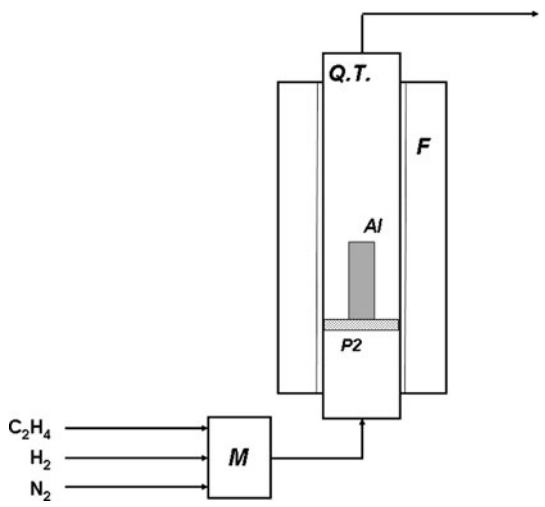


**Fig. 1** Schematic flow sheet of CVD reactor. *M* gas mixer, *Q.T* quartz tube, *F* furnace, *P2* porous gas distributor, *Al* aluminium sample

the samples after growth of CNT by using a high precision balance with a measurements resolution of $10^{-6}$ g. MWCNTs on aluminium were characterized for morphology by using transmission electron microscopy (TEM, JEOL 2010) and scanning electron microscopy (SEM, Zeiss EVO 50 EP), for purity by thermogravimetric analysis (TGA, SDT Q600, from 30 to 900 °C at 10 °C $min^{-1}$) and for surface area by Brunauer–Emmett–Teller analysis with nitrogen gas (BET, ASAP 2010, Micromeritics).

### Electrochemical measurements

The electrochemical properties of the CNTs electrodes were investigated by cyclic voltammetry (CV) in a standard three-electrode cell. CV measurements were performed by a potentiostat/galvanostat (AMEL Mod. 7050). Two types of electrolyte were used for CV, an 1.0 M $H_2SO_4$ aqueous solution and an organic solution having the composition reported in Table 2. A dimension stable anode (DSA) counter electrode along with a saturated calomel reference electrode (SCE) completed the cell set-up. CV measurements on CNT electrodes were made in the potential range between 0 and 1 V vs. SCE at scan rates of 20, 50 and 100 mV $s^{-1}$. Measurements were made at room temperature. The CNT electrode was characterized by impedance spectroscopy in open circuit condition in a three electrodes mode, using an AMEL frequency response analyzer coupled with an AMEL potentiostat, model 7050. Impedance measurements were performed in an 0.1 M $Na_2SO_4$ electrolyte at room temperature with an ac amplitude of 10 mV. Data were collected in the frequency range from $10^5$ to $10^{-1}$ Hz.

## Results and discussion

### Morphology by SEM and TEM

All the conditions experimented for nickel thin film electrodeposition were subsequently tested in CNT growth. The optimum conditions for nickel catalyst electrodeposition were selected primarily according to the visual appearance of the samples, by observing the degree of coverage and the distribution uniformity of the nickel film, then, after CNT deposition, according to the mechanical adhesion of the CNT layer to the substrate and the mass of CNT deposited in 10 min. The conditions selected for nickel deposition were as follows: 60 °C, pH 2, 10 min deposition time, and current density of 10 mA $cm^{-2}$.

**Table 2** Composition of the organic electrolyte for cyclic voltammetry measurements

| Reagent | Mass/g |
|---|---|
| Glycol ethylene | 1,000 |
| Adipic acid | 200 |
| Boric acid | 150 |
| Ammonium hydrate | 178 |
| Water | 500 |

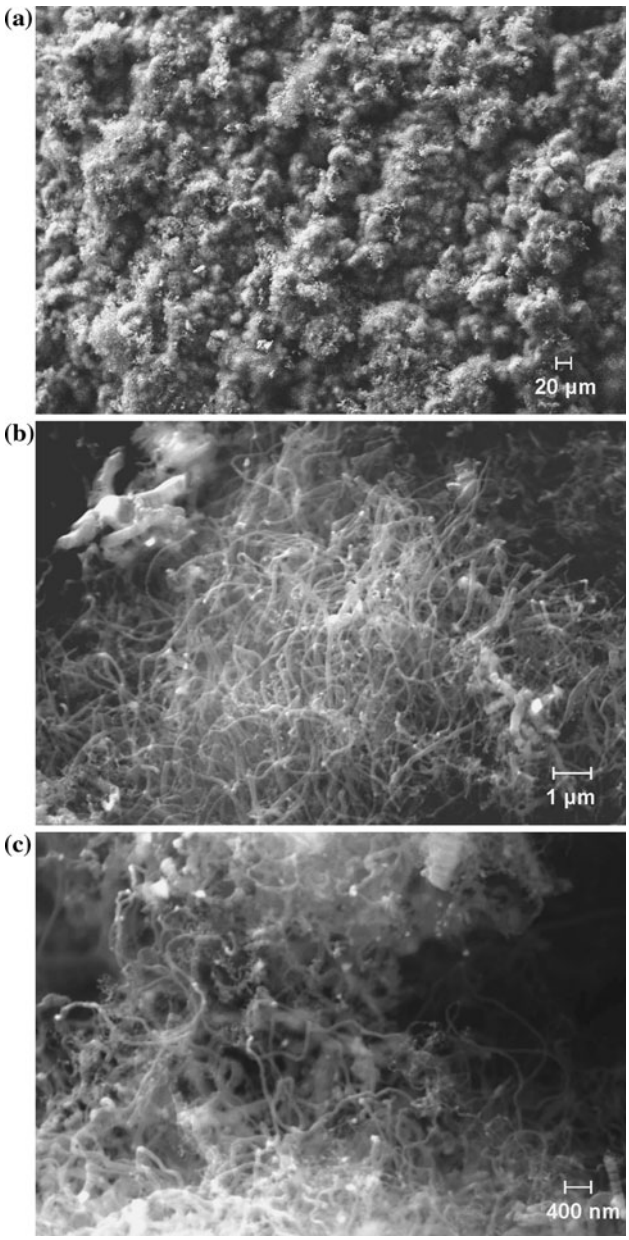


**Fig. 2** SEM micrographs of CNT grown on nickel-plated aluminium substrate: **a** surface morphology of the as-grown layer in **b** and **c** details of the inner layer structure showing bundles of CNT and carbon fibres

Typical SEM and TEM micrographs of the produced CNTs are shown in Figs. 2 and 3, respectively. The CNT layer shows a granular-like appearance resulting from the formation of closely spaced, relatively large bundles of

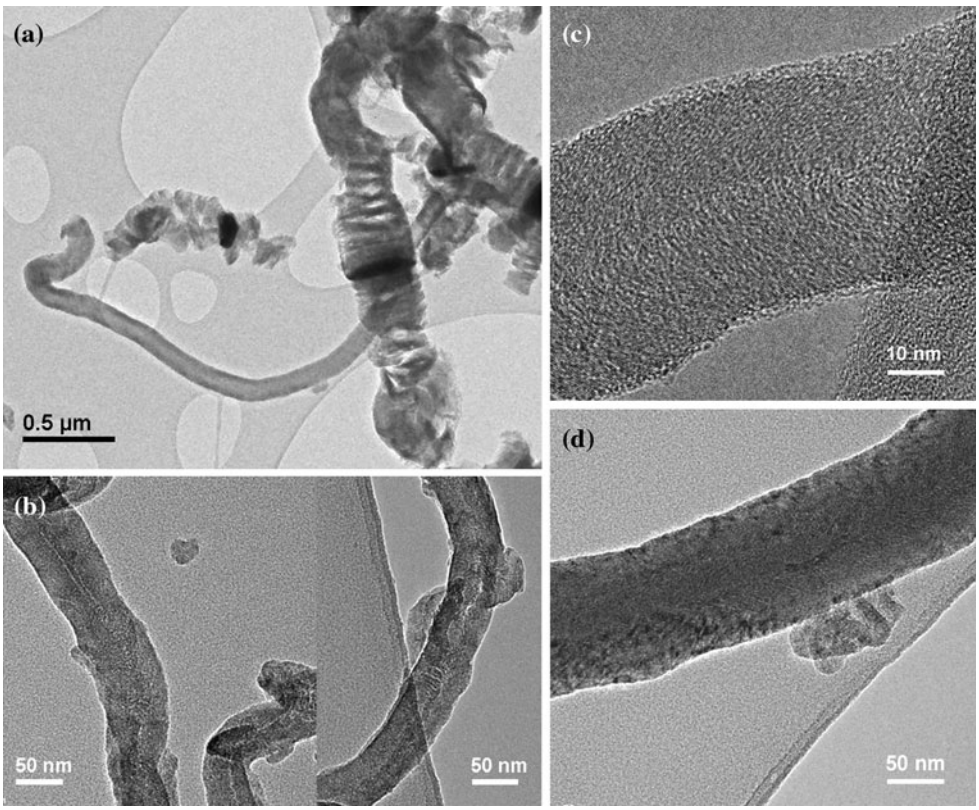


**Fig. 3** TEM micrographs of CNT grown on nickel-plated aluminium substrate: **a** low magnification micrograph showing the presence of nanotubes and filaments made of stacks of parallel lamellae; **b** thick wall and large diameter nanotubes

entangling nanotubes. The CNT bundles give rise to a porous layer decorated at the surface by a dense arrangement of flakes formed by loosely packed CNT, as depicted in Fig. 2. TEM observation disclosed further characteristics of the CNT layer, see Fig. 3. The CNTs grown on aluminium foil were found to be multi-walled with outer diameter ranging from 50 to over 100 nm, and a small hollow core with diameter in the range from 5 to 30 nm. The walls of the CNT had a relatively large thickness, in the range of 20–50 nm, scaling with their diameter, and were apparently formed by non-continuous graphitic layers. The length of CNT was in the order of tens of micrometers. Furthermore, metal particles having size in the range of 10–20 nm, originating from the nickel catalyst film, were detected both in the interior channel and on the walls of CNT.

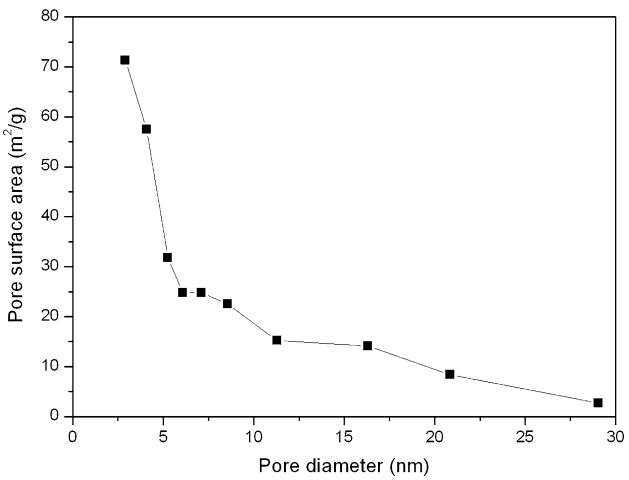


**Fig. 4** Pore size distribution of a CNT electrode

## BET analysis

The specific surface area and average pore diameter of CNT were determined by the BET analysis (Fig. 4). The BET surface area of the CNTs was measured to be 120 $m^2\ g^{-1}$ in substantial agreement with the expected result for MWCNT [16]. On the other hand, this value is much smaller compared to that for activated carbon (1000–2000 $m^2\ g^{-1}$). Theoretically, the higher the specific surface area of an activated carbon the higher the specific capacitance should be. However, the theoretical capacitance of activated carbon is not in good agreement with the observed value, because a significant fraction of the surface area remains in the micropores (<2 nm), which are not accessible to the electrolyte ions [5]. Obviously, both the pore size distribution and the surface area are important factors influencing the electric double-layer capacitance.

According to IUPAC classification [17], there are three classes of pore size: (i) micropores of internal width <2 nm, (ii) mesopores of internal width between 2 and 50 nm and

(iii) macropores of internal width >50 nm. According to the present results, the total volume of pores is 0.149 $cm^3\ g^{-1}$, the pore size distribution is in a range from about 2.5 nm to about 25 nm and the mean pore diameter is between 4 and 7 nm. Apparently, pore is distributed as mesopores according to IUPAC classification. In general, it is known that the pore size in the range of 3–5 nm is required to maximize the capacitance in EDLC [6].

## Thermogravimetry

Since different forms of carbon other than CNT were apparently present, the purity was further characterized by thermogravimetry. The purpose of the thermogravimetric analysis was to assess the purity of CNT according to the difference in oxidation temperature between different forms of carbon materials [17]. In general, there is no a unique combustion temperature of CNT, but the burning temperature is higher for SWCNT (700–800 °C) and lower for MWCNT (600–750 °C), whilst for amorphous carbon is even less (440 °C). Figure 5 shows that, following water loss, a decrease in the mass of the sample under analysis was detected during heating starting from 426 °C. The MWCNTs were completely burned above 600 °C and the remaining material was the nickel catalysts particles. The differential TGA shows a first peak at 130 °C, which is related to water loss, and two other peaks at 510 and 568 °C, which are related to different types of CNT. From these results it may be inferred that CNT are not of the highest quality probably because of the relatively low temperature used for the CVD growth, which was 600 °C instead of the optimum value of 650 °C [17].

## Electrochemical characterization

CV was performed on the CNT electrodes in an organic electrolyte, whose composition in reported in Table 2 and 1.0 M $H_2SO_4$ electrolyte at scan rate of 100, 50, and 20 mV $s^{-1}$. Voltammetric curves at the CNTs electrodes, as shown in Fig. 6, indicate for the electrodes a capacitive charging and discharging behaviour across the spanned potential range from 0 to 1 V versus SCE. The shape of the voltammograms is accordingly near-rectangular, in agreement with previous observation on CNT electrodes, e.g. [18], and the shape is maintained irrespective of the scan rate within the range tested.

In the aqueous electrolyte a slightly decreasing trend of the anodic current results with cycling in the range of potential in excess of about 0.4 versus SCE, which could be related to oxidation of the catalyst nickel film (see graph below in Fig. 6).

The capacitance was derived from the cyclic voltammogram curves using the equation $C = I/(\mathrm{d}V/\mathrm{d}t)$, where $I$ and $\mathrm{d}V/\mathrm{d}t$ are the current and potential scan rate, respectively. The average specific capacitance was obtained by integrating positive and negative current over the CV curves. The calculated specific capacitance for CNT electrode is as high as 79 and 54 F $g^{-1}$ in organic and aqueous electrolyte, respectively.

Table 3 shows the influence of scan rate and electrolyte solution on the specific capacitance of the CNTs electrode. In all cases, the specific capacitance increases with decreasing scan rate and, as already noticed, was lower in the aqueous electrolyte than in the organic electrolyte. The scan rate sensitivity of the specific capacitance is an

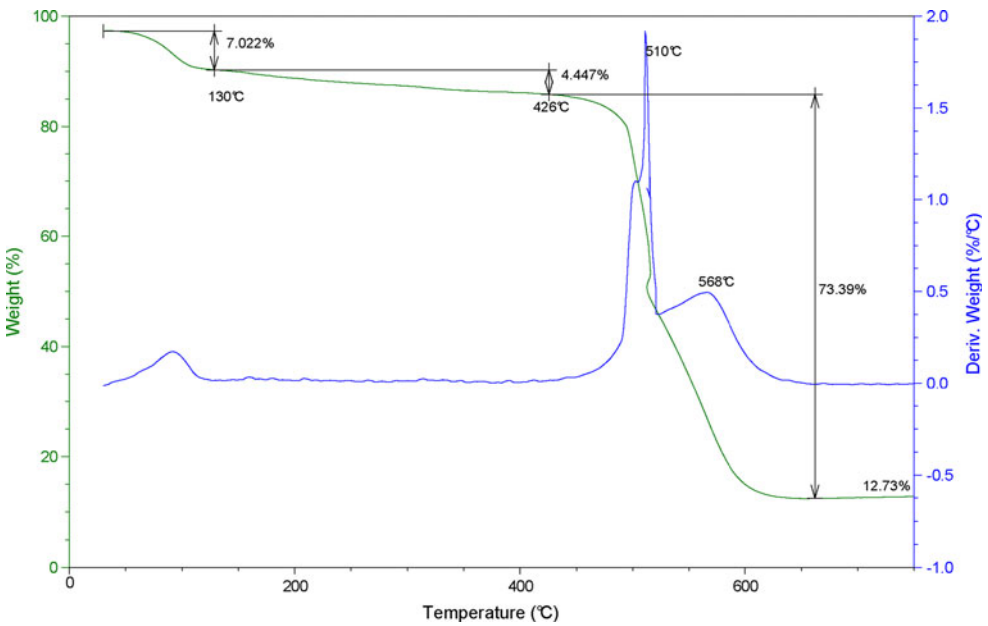


**Fig. 5** Thermogravimetric analysis of raw MWCNT synthesized at 600 °C

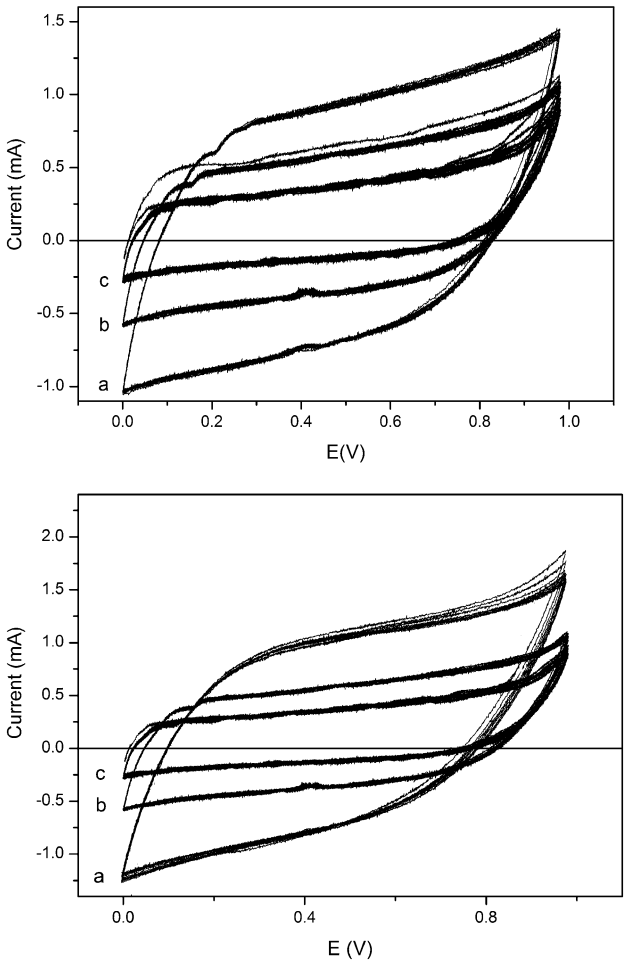


**Fig. 6** Cyclic voltammograms of CNT electrode at scan rates of (a) 100, (b) 50 and (c) 20 mV $s^{-1}$ in organic (*above*) and aqueous (*below*) electrolyte, at room temperature

**Table 3** Influence of scan rate and electrolyte on the specific capacitance of CNT electrode

| Scan rate (mV $s^{-1}$) | Capacitance (F $g^{-1}$) | |
|---|---|---|
| | 1.0 M $H_2SO_4$ | Organic electrolyte |
| 20 | 68 | 94 |
| 50 | 63 | 87 |
| 100 | 54 | 79 |

indirect confirmation of the mixed microporous and mesoporous nature of the CNT active layer [19].

In order to characterize the cyclic behaviour of electrodes, CNT electrodes were subjected to charge/discharge tests at scan rate of 200 mV $s^{-1}$ for 500 cycles in both aqueous and organic solutions. Figure 7 shows the effect of different charge discharge cycle on specific capacitance of the CNT electrode. In both solutions, the specific capacitance of the CNT electrode decreased with an increasing

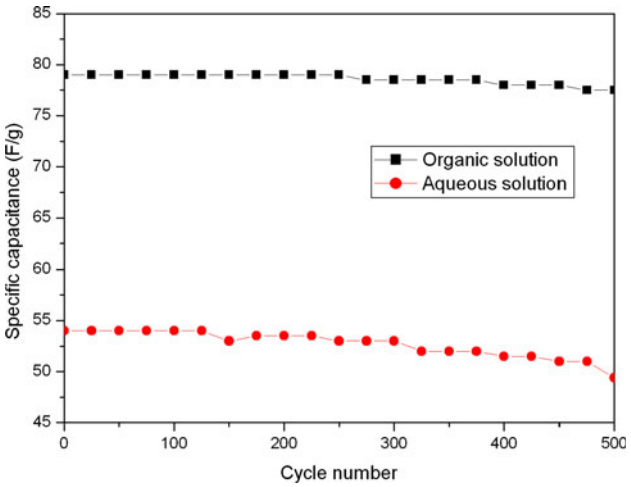


**Fig. 7** Specific capacitance as a function of cycle number in organic and aqueous electrolyte at room temperature

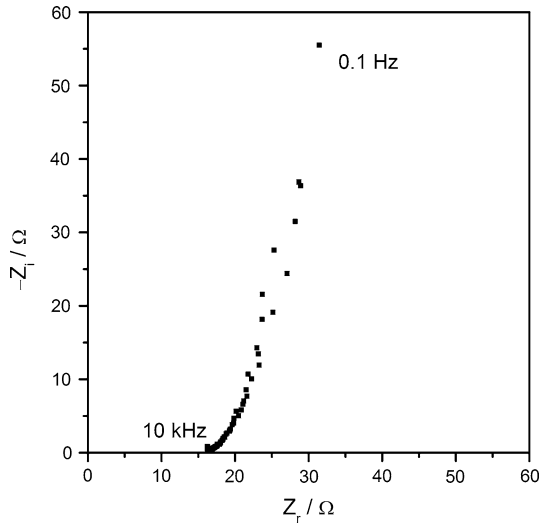


**Fig. 8** Impedance spectrum from 0.1 Hz to 10 kHz recorded in three electrodes mode at a CNT electrode in 0.1 M $Na_2SO_4$ electrolyte

number of charge–discharge cycles. The electrode performed better in the organic solution, showing 2% decrease in the initial capacitance value after 500 cycles. On the other hand, a 9% decrease in the initial capacitance for the CNT electrode in 1.0 M $H_2SO_4$ after 500 cycles was recorded.

A preliminary impedance study of the CNT electrode behaviour was performed in order to confirm its potential as a supercapacitor electrode. The impedance measurements were performed in an 0.1 M $Na_2SO_4$ electrolyte, which accounts for the high observed uncompensated resistance in the impedance spectrum reported in Fig. 8. The impedance spectrum shows a good capacitor like behaviour, i.e. the limit capacitance at the low frequencies, and a relatively small diffusion limitation, i.e. the straight

line which represents the diffusion process in the porous layer at the higher frequencies. Values of the limit capacitance in the range from 50 to 70 F $g^{-1}$ derived from impedance spectra shows a reasonable agreement with the value obtained from CV measurements in the sulphuric acid aqueous electrolyte.

## Conclusions

CNTs were directly grown by CVD on a nickel-plated high purity aluminium substrate as a novel approach to the manufacturing of CNT electrodes for supercapacitors. The as-grown CNT are multi-walled, with diameters between 50 and 100 nm and length of tenths of micrometers, forming a thick and adherent layer made of relatively large bundles. The microstructure of the CNTs layer provides a high surface area along with a high volume of mesopores, resulting in a high value of the specific capacitance of the electrode, as revealed by CV (54 F $g^{-1}$ in aqueous electrolyte and 79 F $g^{-1}$ in organic electrolyte) and confirmed by impedance analysis. Further evidence in support of the viability of the present approach was gained from a preliminary assessment of the cyclability of the electrode.

In conclusion, it was shown that CNT electrodes can be prepared by the direct deposition of the active material on an aluminium substrate. The present approach may be a promising method for the development of CNT-based electrode for supercapacitors. The direct growth of CNT on the current collector can have, in principle, two major implications: the reduction of the contact resistance between the metal support and the active material; and the reduction of the resistivity of the electrolyte within the electrode itself. These are the dominant components of the series resistance that limits the specific power of standard supercapacitors. Eventually, potential future development can be envisaged according to different strategies, such as tailoring of the growth morphology of the CNT and the application of oxidation treatment aimed at increasing the specific capacitance of the electrodes.

**Acknowledgements** We would like to thank Dr. Michele Curioni (School of Materials, The University of Manchester, UK) for TEM analysis and for his comments and remarks. Thanks are also due to Dr. Luca Primavesi (Itelcond s.r.l. Italy) for useful discussions.

## References

1. Conway BE (1999) Electrochemical supercapacitors: scientific fundamentals and technological applications. Plenum Publishers, New York
2. Obreja VN (2008) Physica E 40:2596
3. Kotz R, Carlen M (2000) Electrochim Acta 45:2483
4. Burke A (2000) J Power Sources 91:37
5. Emmenegger CH, Maurona Ph, Sudan P, Wenger P, Hermann V, Gallay R (2003) J Power Sources 124:321
6. Simon P, Gogotsi Y (2008) Nat Mater 7:845
7. Chen JH, Li WZ, Wang DZ, Yang SX, Wen JG, Ren ZF (2002) Carbon 40:1193
8. Gao L, Peng A, Wang Z, Zhang H, Shi Z, Gu Z (2008) Solid State Commun 146:380
9. Kong L-B, Zhang J, An J-J, Luo Y-C, Kang L (2008) J Mater Sci 43:3664. doi:10.1007/s10853-008-2586-1
10. Zhang H, Zhou W, Du Y, Xu J, Yang P (2010) J Mater Sci 45:5795. doi:10.1007/s10853-010-4654-6
11. Hsieh CT, Chou YW, Chen WY (2008) J Solid State Electrochem 12:663
12. Jung M, Kim HG, Lee JK, Joo OS, Mho S (2004) Electrochim Acta 50:857
13. Lin CC, Yang CL (2010) J Electrochem Soc 157(2):A237
14. Lin CC, Huang WF (2010) J Electrochem Soc 157(2):A209
15. Nunga SP, Tito AC, Bianco F, Bestetti M, Mazzocchia V (2009) In: 12nd SFGP Conf., Marseille, France, pp 617–623
16. Peigney A, Laurent C, Flahaut E, Bacsa RR, Rousset A (2001) Carbon 39:507
17. Sing KSW, Everett DH, Haul RAW, Mouscou L, Pierotti RA, Rouquerol J (1985) Pure Appl Chem 57:603
18. Frackowiak E, Béguin F (2001) Carbon 39:937
19. Yang K, Yiacoumi S, Tsouris C (2003) J Electroanal Chem 540:159